A Soft Decision-Directed Blind Equalization Algorithm

Jeyhan Karaoğuz

Center for Communications and Signal Processing
Department of Electrical and Computer Engineering
North Carolina State University

TR-91/16
October 1991

A Soft Decision-Directed Blind Equalization Algorithm

by

JEYHAN KARAOĞUZ

North Carolina State University,
Center for Communications and Signal Processing,
Department of Electrical and Computer Engineering,
P.O.Box 7914, Raleigh, NC, 27695.
(919) 515-5348.

Abstract

A new approach to decision-directed (DD) blind equalization is introduced based on a neural network classification technique. The new DD algorithm, termed soft decision-directed equalization algorithm, is most effective for reconstructing PSK and QPSK signals. It can also be extended to higher order QAM signals at the expense of computational complexity. We show that previously published DD type equalization algorithms reduce to the standard DD equalization algorithm when PSK or QPSK type signals are used. It is known that the standard DD algorithm does not guarantee convergence for closed eye situations. Therefore, the new soft DD algorithm becomes an attractive solution for reconstructing low order QAM signals such as PSK and QPSK. In the simulations, the performance of the soft DD algorithm is illustrated by applying it to a two-dimensional digital mobile communication systems. A time-varying multipath fading channel model is used as the transmission medium. The performance of the soft DD blind equalization algorithm is compared to the standard DD algorithm, the maximum-level-error (MLE) algorithm, the fast recursive least squares decision-feedback equalization (FRLS-DFE) algorithm and Godard's blind equalization algorithm. The comparisons illustrate the improvement in performance achievable with the new soft DD equalization algorithm.

This work was supported by the Center for Communications and Signal Processing, North Carolina State University, Raleigh, NC, 27695-7911.

I. Introduction

The adaptive equalization technique in which the training sequence is replaced by the quantized values of the equalizer output is known as "decision-directed" (DD) equalization [1]. The complex weight vector update equation for a complex DD equalizer, shown in Fig. 1, is given by

$$\mathbf{w}(n+1) = \mathbf{w}(n) - \alpha[y(n) - \hat{y}(n)]\mathbf{r}^*(n) \tag{1}$$

where α is the step size, $y(n)$ and $\hat{y}(n)$ denote the adaptive filter output and the estimate of the decision unit respectively, and $\mathbf{r}^*(n)$ is the complex conjugate of the input data vector stored in the equalizer at time n. The DD blind equalization algorithm has found a wide variety of applications especially in digital radio systems due to its simplicity. However there are two important disadvantages of the DD equalizer: (1) the convergence is slow; (2) the convergence of the DD algorithm can be assured only if the equalizer starts with an "open eye" [2]. These two limitations motivated further research in DD equalization. Sato [3] introduced a new DD blind equalizer based on a coarser quantization scheme. This approach performed better than the standard DD equalization for the "closed eye" situations because the standard algorithm quantizes the output of the equalizer to the nearest data symbol which most likely results in an incorrect decision for channels with severe distortions. Benveniste and Goursat [4] introduced a generalization of Sato's algorithm for complex data symbols. The generalized algorithm had the following update equation:

$$\mathbf{w}(n+1) = \mathbf{w}(n) - \alpha\,[y(n) - \gamma\ \ csign(y(n))]\,\mathbf{r}^*(n). \tag{2}$$

Note that $\hat{y}(n)$ is replaced by $\gamma\ \ csign[y(n)]$ where the complex sign function is defined by $csign(y_r + jy_i) = sgn(y_r) + jsgn(y_i)$. Instead of using the estimate $\hat{y}(n)$, the update relation (2) utilizes the equalizer output quantized to $\gamma\ \ csign[y(n)]$. The scalar γ is given by [4]

$$\gamma = \frac{E\{a_r^2(n)\}}{E\{|a_r(n)|\}} = \frac{E\{a_i^2(n)\}}{E\{|a_i(n)|\}} \tag{3}$$

where $a_r(n)$ and $a_i(n)$ are, respectively, the real and imaginary components of the data symbol $a(n)$. Next, Picchi and Prati [5] introduced a "Stop-and-Go" DD blind equalizer which uses a stop-and-go adaptation rule. This algorithm updates the filter taps according to the standard DD update equation (1) if both the standard DD error "$y(n) - \hat{y}(n)$" and the Sato-like [5] error "$y(n) - \gamma\ \ csign[y(n)]$" have the same sign otherwise the filter taps remain constant. This algorithm

also converged for closed eye situations. Another practical DD blind equalizer was introduced as the Maximum-Level-Error (MLE) algorithm [6]. This algorithm also uses a stop-and-go adaptation rule. The data constellation plane is divided into two regions by a threshold boundary determined by the outermost symbols in the constellation. The adaptation is stopped if the equalizer output is in the interior of the threshold boundary and continued if it is in the exterior of the threshold boundary. For the latter case the sign of the decision directed error is always correct. Therefore the MLE algorithm always updates the filter taps in the correct direction but its disadvantage is that the frequency of updates is small because most of the equalizer outputs fall into the region interior to the threshold boundary. Ross and Taylor [7] slightly modified the MLE algorithm by scaling the magnitude of the update constant instead of stopping the adaptation when the output of the equalizer is in the interior of the threshold boundary.

An interesting and least-mentioned point common to all previously mentioned modified DD algorithms except the MLE algorithm is that they can only be applied to high order constellations such as 16-QAM and 64-QAM. This is because for low order constellations such as PSK and QPSK, Sato's algorithm reduces to the standard DD algorithm. This can be verified if the scalar γ in (3) is calculated for a PSK or QPSK constellation (symmetric around the origin). Then, one can find out that the Sato's estimate "$y(n) - \gamma \ csign[y(n)]$" becomes exactly equal to the standard DD estimate $\hat{y}(n)$ obtained by quantizing the output of the equalizer to the nearest symbol. Consequently, together with the Sato's algorithm the Stop-and-Go algorithm also reduces to the standard DD algorithm because the Sato-like error [5] and the standard DD error becomes equivalent. The PSK and QPSK modulation schemes are important for applications where channel distortions are too severe for reliable operation of higher order constellations. Mobile communication systems is an example where PSK and QPSK modulation schemes are used [8]. Due to the vehicle motion mobile communications channels have rapidly changing fading characteristics which introduce a far more severe distortion than the one introduced by the stationary fading characteristics of the digital radio channels. The only available DD equalization algorithms for reconstructing PSK and QPSK signals are the MLE algorithm which has a very slow convergence rate and the standard DD algorithm which can only guarantee convergence in open eye situations which is not the case for mobile multipath fading channels. In this paper we will introduce a new DD blind equalizer which can converge in closed eye situations. The new algorithm is most effective for reconstructing PSK and QPSK signals. The channel equalization problem is treated as a classification problem. In doing

so, a neural network technique is employed where the transmitted data sequence is reconstructed at the receiver as accurately as possible. The final result of this approach is shown to be a decision-directed equalizer. The new algorithm will be referred to as "soft decision-directed equalizer". The previous modifications [3,4,5] to the standard DD algorithm has been introduced primarily by ad-hoc means. In this paper a theoretical justification is provided in deriving the soft DD equalization algorithm.

II. Derivation of Soft Decision-Directed Equalization Algorithm

In the equations the following definitions hold. The received complex input vector stored in the equalizer taps at time n is represented by $\mathbf{r}$ and defined as

$$\mathbf{r} = \mathbf{x}_i + j\mathbf{y}_i = [r(k) \;\; r(k-1) \;\; \ldots \;\; r(k-N+1)]^t. \tag{4}$$

The blind equalizer is composed of an arbitrary N^{th} order complex FIR filter whose taps are adaptively adjustable. The complex weight vector is given by

$$\mathbf{w} = \mathbf{w}_R + j\mathbf{w}_I = [w_0(k) \;\; w_1(k) \;\; \ldots \;\; w_{N-1}(k)]^t. \tag{5}$$

The soft decision-directed blind equalizer for 2-D communication systems is shown in Fig. 1. The blind equalizer output is

$$y(k) = x_o + jy_o = \mathbf{r}^t\mathbf{w}. \tag{6}$$

All boldface variables denote vectors.

When digital data is transmitted through an ideal channel, the reconstructed constellation at the receiver will be composed of single points corresponding to each complex symbol in the alphabet. However, for practical dispersive channels, the detected data sequence forms a constellation with clusters instead of single points as depicted in Fig. 2 for a QPSK scheme. The variances of the clusters depend on the distortion introduced by the channel. Our neural network technique employs the Gaussian cluster formation algorithm [9] which models each cluster by a Gaussian distribution with *apriori* known mean and variance, and classifies the incoming data as belonging to one of these clusters. For a common dispersive channel such as a fading multipath channel, the Gaussian model can be justified as follows. The transmitted symbols can be taken as independent random variables. Each symbol travels via energy spread over a random number of unequal length paths, and at the receiver all of the multipath signals are combined. By the "central limit theorem"

the distribution of the summation of random variables approaches a Gaussian distribution as the number of the paths increases.

Let us consider one of the clusters (for example "Cluster I") in the constellation diagram (Fig. 2). The transmitted complex symbol corresponding to "Cluster I" is composed of two random components (x, y). Therefore the joint Gaussian distribution $f(x, y)$ which models "Cluster I" takes on the following form

$$f(x,y) = \frac{1}{2\pi|K|^{1/2}} \exp(-\frac{1}{2}\mathbf{r}^t K^{-1}\mathbf{r}) \tag{7}$$

where $\mathbf{r} = [(x-\mu_x),(y-\mu_y)]^t$. The μ_x and μ_y specify the mean values of "Cluster I" with respect to x-axis and y-axis respectively. The covariance matrix K is defined as

$$K = E\left\{\begin{bmatrix} (x-\mu_x)^2 & (x-\mu_x)(y-\mu_y) \\ (x-\mu_x)(y-\mu_y) & (y-\mu_y)^2 \end{bmatrix}\right\}. \tag{8}$$

In 2-D communication systems the random symbol components x and y are statistically independent, therefore K becomes

$$K = \begin{bmatrix} \sigma_x^2 & 0 \\ 0 & \sigma_y^2 \end{bmatrix} \tag{9}$$

and the determinant of K becomes

$$|K| = \sigma_x^2 \sigma_y^2. \tag{10}$$

Hence assuming independent real and imaginary components (x, y) for each symbol, the joint Gaussian distribution takes on the following form

$$f(x,y) = \frac{1}{2\pi\sigma_x\sigma_y} \exp\left(-\frac{1}{2}\left[\frac{(x-\mu_x)^2}{\sigma_x^2} + \frac{(y-\mu_y)^2}{\sigma_y^2}\right]\right) \tag{11}$$

where (μ_x, σ_x^2) and (μ_y, σ_y^2) are the mean and variance pairs for the real and imaginary parts of the transmitted symbol corresponding to "Cluster I".

We now extend (11) to define a general performance function which models the entire data constellation encompassing all the clusters (assuming there are n of them, for example for QPSK n=4, for 64-QAM n=64).

$$\Psi = \log\left[\sum_n \frac{p_n}{2\pi\sigma_{x_n}\sigma_{y_n}} \exp\left(-\frac{1}{2}\left[\frac{(x_o-\mu_{x_n})^2}{\sigma_{x_n}^2} + \frac{(y_o-\mu_{y_n})^2}{\sigma_{y_n}^2}\right]\right)\right] \tag{12}$$

where the index n goes through all the clusters. The log operation is performed to make Ψ have a smoother performance surface which is convenient for optimization purposes. The $x_o + jy_o$ is the

complex output of the blind equalizer as shown in Fig. 1. Substituting (4) and (5) in (6), the real and imaginary parts of the equalizer output x_o and y_o respectively, can be found as

$$\begin{aligned} x_o &= \mathbf{x}_i^t \mathbf{w}_R - \mathbf{y}_i^t \mathbf{w}_I \\ y_o &= \mathbf{y}_i^t \mathbf{w}_R + \mathbf{x}_i^t \mathbf{w}_I. \end{aligned} \tag{13}$$

Notice that if (13) is substituted in (12) Ψ becomes a function of the real and imaginary parts of the equalizer filter weight vector $\mathbf{w}_R, \mathbf{w}_I$ respectively. The algorithm modifies the complex weights of the FIR filter to maximize the log likelihood of generating the observed output values from the mixture of Gaussian distributions in (12). If we view the output of the blind equalizer as a data point, the algorithm maximizes $\Psi(\mathbf{w}_R, \mathbf{w}_I)$ by moving the data point toward the center of the nearest cluster. The p_n in (12) is the proportion of the n^{th} cluster in the mixture. For practical 2-D data communication systems the p_n's can be taken as equal since the symbols are chosen equally likely from an alphabet. In addition, we can impose the same variance σ^2 for each cluster. After making these assumptions (12) reduces to

$$\Psi(\mathbf{w}_R, \mathbf{w}_I) = \log \left[\sum_n \exp \left(-\frac{1}{2\sigma^2} \left[(x_o - \mu_{x_n})^2 + (y_o - \mu_{y_n})^2 \right] \right) \right] \tag{14}$$

where each cluster has a mean value defined by the pair (μ_{x_n}, μ_{y_n}) and a variance specified by σ^2.

To maximize (14) with respect to the complex FIR weight vector, we compute the gradient ascent in $\Psi(\mathbf{w}_R, \mathbf{w}_I)$. An LMS-like stochastic gradient update algorithm is employed because of its stability, robustness and ease of implementation. After applying it to the complex FIR weights [10], one obtains

$$\mathbf{w}_R(k+1) = \mathbf{w}_R(k) + \alpha \frac{\partial \Psi(\mathbf{w}_R, \mathbf{w}_I)}{\partial \mathbf{w}_R} \tag{15}$$

$$\mathbf{w}_I(k+1) = \mathbf{w}_I(k) + \alpha \frac{\partial \Psi(\mathbf{w}_R, \mathbf{w}_I)}{\partial \mathbf{w}_I} \tag{16}$$

where α is the learning rate. The $\mathbf{w}_R(k)$ and $\mathbf{w}_I(k)$ are the real and imaginary parts of the complex FIR weight vector at time k. Notice that all complex linear unit weights are updated simultaneously after each iteration proportional to gradient ascent in $\Psi(\mathbf{w}_R, \mathbf{w}_I)$ with respect to weights. The vector partial derivatives can be written as

$$\frac{\partial \Psi(\mathbf{w}_R, \mathbf{w}_I)}{\partial \mathbf{w}_R} = \frac{(1/\sigma^2)}{\sum_n \Psi_n} \sum_n \left[(\mu_{x_n} - x_o) \frac{\partial x_o}{\partial \mathbf{w}_R} + (\mu_{y_n} - y_o) \frac{\partial y_o}{\partial \mathbf{w}_R} \right] \Psi_n \tag{17}$$

$$\frac{\partial \Psi(\mathbf{w}_R, \mathbf{w}_I)}{\partial \mathbf{w}_I} = \frac{(1/\sigma^2)}{\sum_n \Psi_n} \sum_n \left[(\mu_{x_n} - x_o) \frac{\partial x_o}{\partial \mathbf{w}_I} + (\mu_{y_n} - y_o) \frac{\partial y_o}{\partial \mathbf{w}_I} \right] \Psi_n \tag{18}$$

where

$$\Psi_n = \exp\left(-\frac{1}{2\sigma^2}\left[(x_o - \mu_{x_n})^2 + (y_o - \mu_{y_n})^2\right]\right). \tag{19}$$

Assuming a QPSK constellation as illustrated in Fig. 2, four symbols are located symmetrically around the origin. Using (13), after some algebraic manipulations, the partial derivatives can be written as

$$\frac{\partial\Psi(\mathbf{w}_R, \mathbf{w}_I)}{\partial\mathbf{w}_R} = -\frac{1}{\sigma^2}\sum_{m=1}^{2}\sum_{n=1}^{2}\Omega_{mn}(x_o, y_o)\left[(x_o - \mu_m)\mathbf{x}_i + (y_o - \mu_n)\mathbf{y}_i\right] \tag{20}$$

$$\frac{\partial\Psi(\mathbf{w}_R, \mathbf{w}_I)}{\partial\mathbf{w}_I} = -\frac{1}{\sigma^2}\sum_{m=1}^{2}\sum_{n=1}^{2}\Omega_{mn}(x_o, y_o)\left[(y_o - \mu_n)\mathbf{x}_i - (x_o - \mu_m)\mathbf{y}_i\right] \tag{21}$$

and

$$\Omega_{mn}(x_o, y_o) = \frac{1}{\left(1 + \exp(-\frac{2\mu_m x_o}{\sigma^2})\right)\left(1 + \exp(-\frac{2\mu_n y_o}{\sigma^2})\right)} \tag{22}$$

where $\mu_n = (-1)^n\mu$ and μ is the symmetric mean, and $\sum_{m=1}^{2}\sum_{n=1}^{2}\Omega_{mn}(x_o, y_o) = 1$. The real and imaginary components of the weight vector are initialized to zero except for the real component of the first tap which is initialized to 1. The update equations (15,16) continuously adjust the complex weight vector so that the output of the blind equalizer forms four clusters where the clusters have mean and variance values specified by $(\mu_m, \mu_n : m, n = 1, 2)$ and σ^2 respectively.

Before elaborating on the final result (20,21,22) of the soft DD algorithm, we will show that the standard DD update equation (1) is a special case of the soft DD algorithm's update equations (20,21). Again consider the QPSK data constellation as shown in Fig. 2, and assume that the real and imaginary parts of the equalizer output x_o, y_o are each greater than zero. Accordingly, the four exponentials in equation (14) (for QPSK n=4) take different values. For the moment ignore the smaller exponentials and keep the largest one corresponding to the positive mean values $\mu_x = \mu_y = \mu$. This is equivalent to ignoring the probability that the particular output value can be from the clusters farther away. Therefore (14) reduces to

$$\Psi(\mathbf{w}_R, \mathbf{w}_I) = -\frac{1}{2\sigma^2}\left[(x_o - \mu)^2 + (y_o - \mu)^2\right]. \tag{23}$$

Furthermore, the partial derivatives can be written as

$$\frac{\partial\Psi(\mathbf{w}_R, \mathbf{w}_I)}{\partial\mathbf{w}_R} = -\frac{1}{\sigma^2}\left[(x_o - \mu)\mathbf{x}_i + (y_o - \mu)\mathbf{y}_i\right] \tag{24}$$

$$\frac{\partial\Psi(\mathbf{w}_R, \mathbf{w}_I)}{\partial\mathbf{w}_I} = -\frac{1}{\sigma^2}\left[(y_o - \mu)\mathbf{x}_i - (x_o - \mu)\mathbf{y}_i\right]. \tag{25}$$

The updates (20,21) for the real and imaginary parts of the weight vector reduce to the standard DD updates (24,25) where the mean values of the real and imaginary parts of the equalizer output are used as the estimates in (1). If you substitute (24,25) in (15,16) the result becomes equivalent to the standard DD equation (1) except for a normalization factor σ^2. Therefore the soft DD algorithm is equivalent to the standard DD algorithm if we ignore the probability that the equalizer output can be from the clusters farther away. With this assumption, we place full confidence in the blind equalizer output estimate as does the standard DD equalizer. However the estimates for the "closed-eye" situations are most likely incorrect. Therefore as proved in [2], the standard DD algorithm may not converge since the incorrect decisions move the weight vector in the wrong direction.

The final result of the proposed algorithm is the set of the equations (20,21,22). Recall that these equations were derived from (14) by taking into account the fact that any given equalizer output value can be from any one of the clusters in the constellation. Therefore, the update equations (20,21) are the sum of 4 decision-directed updates corresponding to 4 clusters in the QPSK constellation. The probability that an output belongs to a certain cluster is determined by the joint sigmoid function $\Omega_{mn}(x_o, y_o)$ in (22) which can take values between 0 and 1. This decision procedure is analogous to the Bayes decision rule used in [11]. The probability that a given equalizer output can be from the clusters farther away is taken into account however the clusters that are farther away from the given equalizer output have relatively less effect than the ones closer in updating the filter weights. Therefore, the joint sigmoid function $\Omega_{mn}(x_o, y_o)$ introduces a soft-decision as to which cluster a given output most likely belongs to, rather than an unreliable hard-decision made by the standard DD algorithm. Now let us see what improvement is achieved by the soft-decision capability of the new algorithm instead of the hard-decision employed by the standard DD algorithm. Consider the case when the equalizer output is near zero. For the QPSK constellation described above, the standard DD algorithm most likely makes an incorrect decision because the output value can be from any one of the four clusters. The disadvantage of the standard DD algorithm is that the weights are changed by (24,25) the most for these highly ambiguous estimates. Consequently, most of the time the filter taps are updated in the wrong direction by a large amount. This phenomenon causes the standard DD equalizer to diverge for closed eye situations where there are many ambiguous decisions to make. On the other hand, the soft DD algorithm makes very small changes in the weight vector for the cases when the equalizer output is near zero. For these highly ambiguous cases the terms in the summations in (20,21)

approximately cancel out since each update in (20,21) (corresponding to each cluster) changes the filter weights by the same magnitude but in opposite directions. In other words, when the estimates are found to be unreliable the weight update is virtually stopped. The simulation results in the next section support the line of reasoning presented above. The simulations demonstrate that for closed eye situations where there are many ambiguous decisions to make, the soft DD algorithm successfully converges whereas the standard DD algorithm fails to converge.

III. Simulations and Results

In the simulations we investigated the capabilities of the soft DD blind equalizer and compared it to the standard DD algorithm, the MLE algorithm, the fast recursive least mean squares decision feedback (FRLS-DFE) [12] algorithm and the conventional constant modulus algorithm (CMA) [13] which is a special case of Godard's blind equalizer [14]. The fading channel is composed of four multipath channels with delays up to four times the symbol duration. The received signal at each multipath is composed of forty different scattered signals with random, and mutually statistically independent amplitudes, phases and angles of arrival. Finally, a vehicle speed of 45 mi/hr is applied which results in 60 Hz peak Doppler shift and about 16 ms channel coherence time. This small coherence time causes rapid time-varying fading [15]. The number of taps are 8 for the standard DD, MLE, CMA and soft DD algorithms. For the FRLS-DFE, the number of taps is 30 and 4 for the forward and feedback filters, respectively. Fig. 3 shows the distorted QPSK constellation due to the time-varying fading channel. Evidently, the eye pattern is closed. Fig. 4 illustrates the output of the standard DD algorithm which failed to reconstruct the desired constellation. Fig. 5 is the output of the MLE algorithm where it performed better than the standard DD algorithm but the quality of the equalized constellation is still poor and also the convergence duration is considerably long. Fig. 6 is the output of the FRLS-DFE where the bit-error-rate is still quite high. These results are as expected. Due to the closed eye situation there are many ambiguous cases (symbols mapped around origin in Fig. 3) to decide and any incorrect decision made by the standard DD equalizer moves the equalizer weight vector in the wrong direction and finally causes it to diverge. For the FRLS-DFE algorithm, the incorrect decisions not only moves the weight vector in the wrong direction but also causes error propagation in the feedback filter [8] which results in the poor performance as shown in Fig 6. The output of the CMA is illustrated in Fig. 7. Evidently, the objective function of the CMA which seeks a constant modulus for the output is not suitable for the

fading channel as the resulting constellation is not well-defined. Fig. 8 presents the output of the new soft DD blind equalization algorithm for the same channel. While the other algorithms failed, the soft DD equalization algorithm successfully reconstructed the QPSK data constellation because of the soft-decision sigmoid function (22) which enables the algorithm to handle the ambiguous and reliable estimates more efficiently. The convergence rate of the soft DD algorithm is compared to other algorithms and illustrated in Fig. 9. A moderate distortion multipath fading channel is used in these simulations in order to ensure the convergence of the standard DD algorithm and the MLE algorithm. Fig. 9 is determined by taking an average of 36 individual runs with different seeds for the random complex binary input. Due to the known training sequence FRLS-DFE converges faster than the other algorithms. The soft DD blind equalization algorithm follows the FRLS-DFE in terms of convergence speed. The standard DD algorithm and the MLE algorithm are the slowest. The convergence rate of the standard DD is slow because wrong decisions delay convergence. The convergence rate of the MLE algorithm is the slowest because it waits for a reliable data to update the filter taps.

IV. Conclusion

A soft decision-directed blind equalization algorithm has been presented. Unlike other DD algorithms [4,5] which reduce to standard DD algorithm for low order QAM applications (such as PSK and QPSK), the new algorithm is most effective for reconstructing PSK and QPSK signals. The proposed algorithm can also reconstruct higher order QAM signals but the computational complexity increases. Simulation results demonstrated that the soft DD blind equalization algorithm performed significantly better than the existing algorithms such as the standard DD algorithm, the MLE algorithm, the FRLS-DFE algorithm and the CMA.

References

[1] J.E. Mazo, "Analysis of Decision-Directed Equalizer Convergence", *The Bell System Journal*, Vol. 59, No. 10, December 1980, pp. 1857-1876.

[2] O. Macchi and E. Eweda, "Convergence Analysis of Self-Adaptive Equalizers", *IEEE Trans. on Inform. Theory*, Vol. 30, 1984, pp. 161-176.

[3] Y. Sato, "A Method of Self-Recovering Equalization for Multilevel Amplitude-Modulation Schemes", *IEEE Trans. on Commun.*, Vol. 23, 1975, pp. 679-682.

[4] A. Benveniste and M. Goursat, "Blind Equalizers", *IEEE Trans. on Commun.*, Vol. 32, No. 8, 1984, pp. 871-883.

[5] G. Picchi and G. Prati, "Blind Equalization and Carrier Recovery Using a "Stop-and-Go" Decision-Directed Algorithm ", *IEEE Trans. on Communications*, Vol. 35, 1987, pp. 877-887.

[6] R. Yatsuboshi, N. Sata, and K. Aoki, "A Convergence of Automatic Equalizer by Maximum Level Error Control," *Nat. Conv. Rec., IECE Japan*, No. 2192, 1974

[7] F.J. Ross, D.P. Taylor, "An Enhancement to Blind Equalization Algorithms," *IEEE Transactions on Communications*, Vol. 39, No. 5, 1991, pp. 636-639

[8] B. Gudmundson, "Adaptive Equalizers with Application to Mobile Radio", *Ph.D Dissertation*, September 1988, Electrical Engineering, Royal Institute of Technology, Sweden.

[9] G.E. Hinton, S.J. Nowlan, "The Bootstrap Widrow-Hoff Rule as a Cluster-Formation Algorithm", *Neural Computation*, No. 2, 1990, pp. 355-362.

[10] B. Widrow et.al., " The Complex LMS Algorithm", *Proc. of the IEEE*, April 1975, pp. 719-720.

[11] S. Chen, G.J. Gibson, C.F.N. Cowan, "Adaptive Channel Equalisation Using a Polynomial-Perceptron Structure", *IEE Proc., Pt. I*, Vol. 137, No. 5, October 1990, pp. 257-264.

[12] T. Adali, S.H. Ardalan, "Multi-Channel General Order Fast Transversal Filter Applied to Rapid Equalization of Fading Mobile Channels", *Submitted to ICASSP'92.*

[13] J. Karaoguz, S.H. Ardalan, "Use of Blind Equalization for Teletext Broadcast Systems", *IEEE Transactions on Broadcasting,* Vol. 37, No. 2, June 1991, pp. 44-54.

[14] D. N. Godard, "Self-Recovering Equalization and Carrier Tracking in Two-Dimensional Date Communication Systems," *IEEE Transactions on Communications*, Vol. COM-28, No. 11, November 1980, pp. 1867-1875.

[15] J. G. Proakis, "Adaptive Equalization for TDMA Digital Mobile Radio", *IEEE Trans. on Vehicular Technology*, Vol. 40, No. 2, May 1991, pp. 333-341.

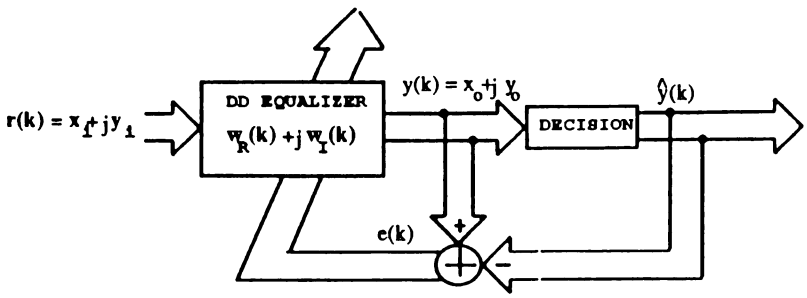

Figure 1: Decision-Directed Blind Equalizer

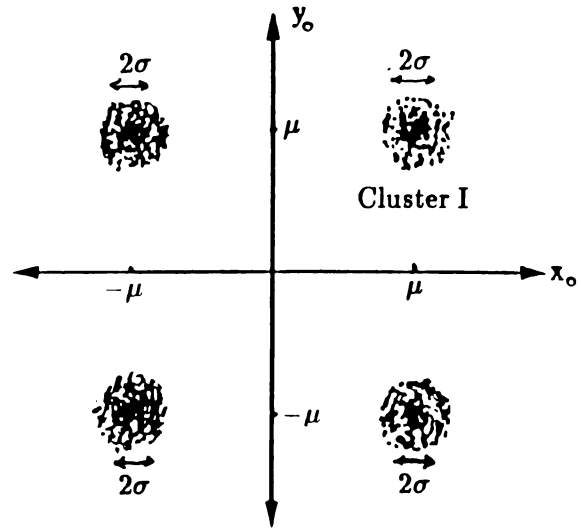

Figure 2: QPSK Data Constellation

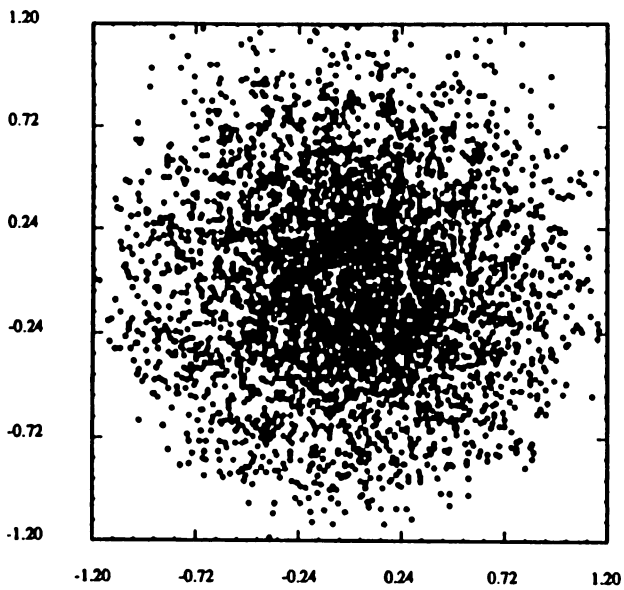

Figure 3: Distorted QPSK Constellation due to Time-Varying Multipath Fading Channel

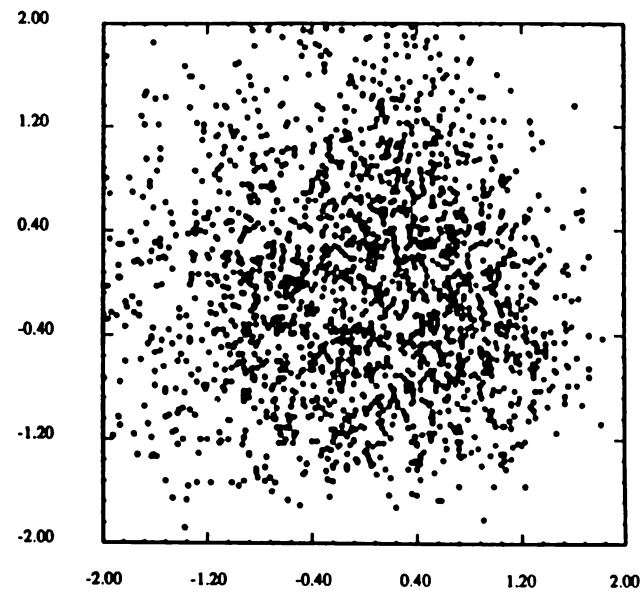

Figure 4: Output of Standard DD Equalizer

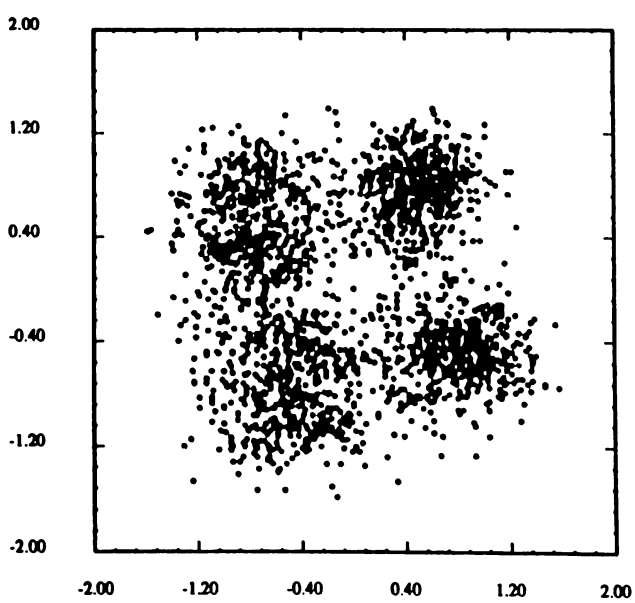

Figure 5: Output of MLE Equalizer

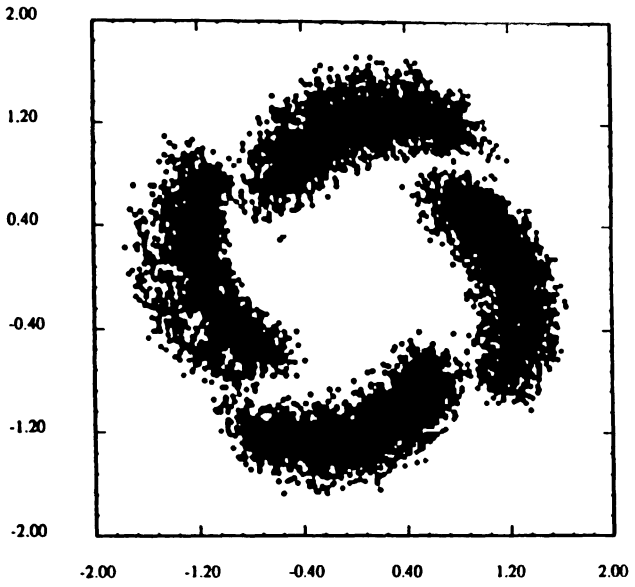

Figure 6: Output of FRLS-DFE

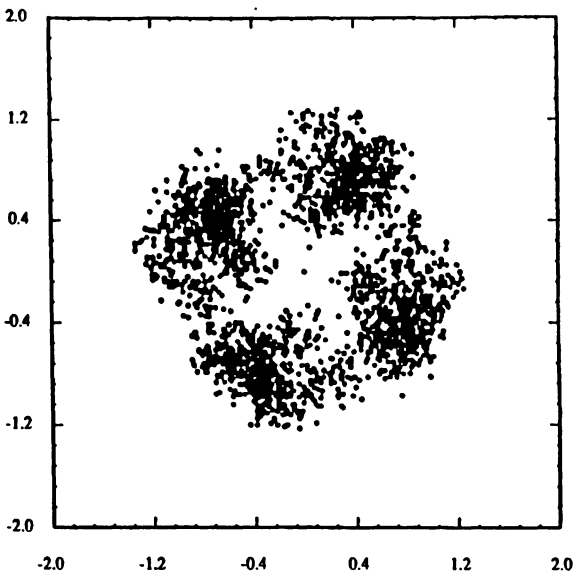

Figure 7: Output of CMA

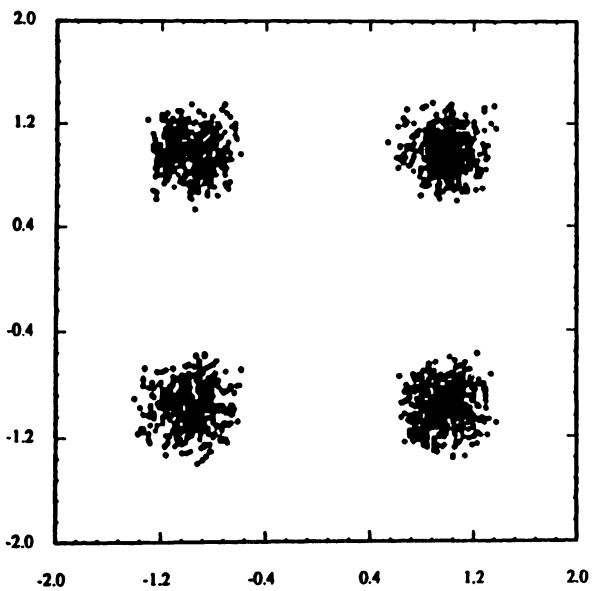

Figure 8: Output of Soft DD Equalizer

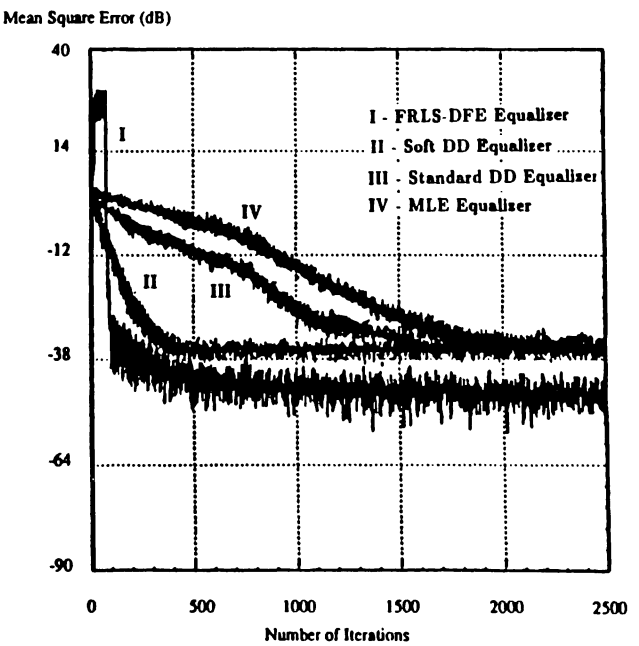

Figure 9: Convergence Rate of Soft DD Equalizer Compared to Other Equalizers